PERGAMON

Journal of Quantitative Spectroscopy & Radiative Transfer 82 (2003) 391–399

Journal of Quantitative Spectroscopy & Radiative Transfer

www.elsevier.com/locate/jqsrt

Submillimeter-wave measurements of the pressure broadening of BrO

M.M. Yamada[a], M. Kobayashi[a], H. Habara[a], T. Amano[a], B.J. Drouin[b,*]

[a] *National Space Development Agency, Institute for Astrophysics and Planetary Sciences, Ibaraki University, 2-1-1 Bunkyo, Mito 310-8512, Japan*

[b] *Jet Propulsion Laboratory, California Institute of Technology, Pasadena, CA 91109-8099, USA*

Received 22 December 2002; received in revised form 20 January 2003; accepted 22 January 2003

Abstract

The N_2 and O_2 pressure broadening coefficients of the $J = 23.5 \leftarrow 22.5$ and $J = 25.5 \leftarrow 24.5$ rotational transitions in the ground vibronic state $X^2\Pi_{3/2}$ of ^{81}BrO at 624.768 and 650.178 GHz have been independently measured at Ibaraki University and Jet Propulsion Laboratory. These lines are expected to be monitored by the superconducting submillimeter-wave limb emission sounder in the Japanese Experiment Module on the International Space Station (JEM/SMILES) as well as the earth observing system microwave limb sounder (EOS-MLS). This work provides temperature-dependent pressure broadening parameters of BrO needed by the space station and satellite based observations. The BrO pressure broadening coefficients and their 1σ uncertainties are: $\gamma_0(N_2) = 3.24 \pm 0.05$ MHz/Torr and $\gamma_0(O_2) = 2.33 \pm 0.06$ MHz/Torr for the 624.768 GHz transition at room temperature (296 K). For the 650.178 GHz line, the results are: $\gamma_0(N_2) = 3.20 \pm 0.07$ MHz/Torr and $\gamma_0(O_2) = 2.41 \pm 0.06$ MHz/Torr. The temperature dependence exponents and their 1σ error are determined to be: $n(N_2) = -0.76 \pm 0.05$ and $n(O_2) = -0.93 \pm 0.07$ for the 624.768 GHz transition, and $n(N_2) = -0.84 \pm 0.07$ and $n(O_2) = -0.70 \pm 0.07$ for the 650.178 GHz transition.

PACS: 33.70.Jg; 33.70. – w; 33.20. – t; 33.20.Bx; 07.57. – c

Keywords: Bromine monoxide; Linewidths; Halfwidths; Pressure broadening; Atmospheric spectra; Lineshape

1. Introduction

The BrO radical is a short-lived species that plays an important role as an intermediate in chemical reaction cycles in the Earth's upper atmosphere [1]. For example, BrO is a catalyst in the destruction cycles of stratospheric ozone. It is well known that the ClO radical is a primary molecule that

* Corresponding author. Fax: +1-818-354-8460.
E-mail addresses: amano@mx.ibaraki.ac.jp (T. Amano), bdrouin@mail2.jpl.nasa.gov (B.J. Drouin).

0022-4073/03/$ - see front matter © 2003 Elsevier Ltd. All rights reserved.
doi:10.1016/S0022-4073(03)00165-1

depletes the ozone layer, but, on the other hand, it is not so well known that the BrO radical also makes an unignorable contribution to this depletion cycle. These important radicals are expected to be monitored by the superconducting submillimeter-wave limb emission sounder, which will be accommodated on the Exposed Facility of the Japanese Experiment Module on the International Space Station (JEM/SMILES) [2], as well as the Earth Observing System Microwave Limb Sounder (EOS-MLS) on board the NASA AURA spacecraft [3]. Both missions will monitor the BrO lines at 624.77 GHz ($J = 23.5 \leftarrow 22.5$) and 650.18 GHz ($J = 25.5 \leftarrow 24.5$) in the ground vibronic state ($X^2\Pi_{3/2}$). Retrieval of reliable temporal and geographic profiles of this radical from atmospheric observations requires temperature-dependent pressure broadening parameters for the chosen rotational transitions determined to within a few percent. Laboratory measurements with this accuracy are often distorted by systematic errors. The rotational lines of BrO have complicated profiles due to the hyperfine and Λ-type doubling interactions. The hyperfine splittings in this frequency region are about the same order of magnitude as the linewidths. These factors pose severe difficulty for measurement of the pressure broadening using conventional methods. For example, fitting of the line profiles to theoretical formula such as the Voigt profile turns out to be futile. However, the convolution-fitting algorithm that was devised by Pickett [4] makes it possible to determine the pressure broadening parameters from the partially resolved multi-line profiles.

There are relatively few measurements of the pressure broadening parameters of BrO in the submillimeter-wave region. Fraser measured the pressure broadening parameter of ^{81}BrO by observing the $J = 27.5 \leftarrow 26.5$ transition with a tunable sideband of a submillimeter-wave laser line (TuFIR) [5]. Bauer et al. retrieved the ^{79}BrO $J = 18.5 \leftarrow 17.5$ pressure broadening at two temperatures using FTFIR [6]. In the present investigation, accurate pressure broadening coefficients of BrO have been obtained for two transitions in the sub-millimeter wavelengths using the convolution method. The temperature dependence of the broadening parameters have also been determined. Due to common inconsistencies in these types of measurements, two laboratories, Ibaraki and JPL, have agreed to independently measure the broadening parameters of these important BrO transitions. Comparison of individual temperature dependencies determined separately with the Ibaraki data and the JPL data are found to be consistent for all but the O_2 broadening of the 624 GHz transition. For this case, the JPL data points at higher temperatures are consistently larger. The individual temperature exponent values differ, but overlap within their respective 3σ uncertainties. In the interests of presenting the best values with the least bias only the combined analysis is reported.

2. Experiment

The measurements at Ibaraki University were carried out using a submillimeter-wave spectrometer that employs Russian-made backward wave oscillators (BWO) as a radiation source [7]. Fig. 1 shows a schematic diagram of the experimental setup at Ibaraki University. The oscillation frequency is phase-locked to harmonics from a Gunn oscillator. A liquid helium cooled InSb detector is used for detection of submillimeter-wave radiation. A “top-hat” frequency modulation scheme with 2f detection is employed for recording the absorption signals.

The Pyrex glass absorption cell is 170 cm long, and 10 cm in diameter. A pair of copper jackets are placed over the middle part of the cell over which copper tubing is soldered. The cell is cooled by flowing chilled methanol from a refrigerated bath circulator (NESLAB ULT-80). The temperature

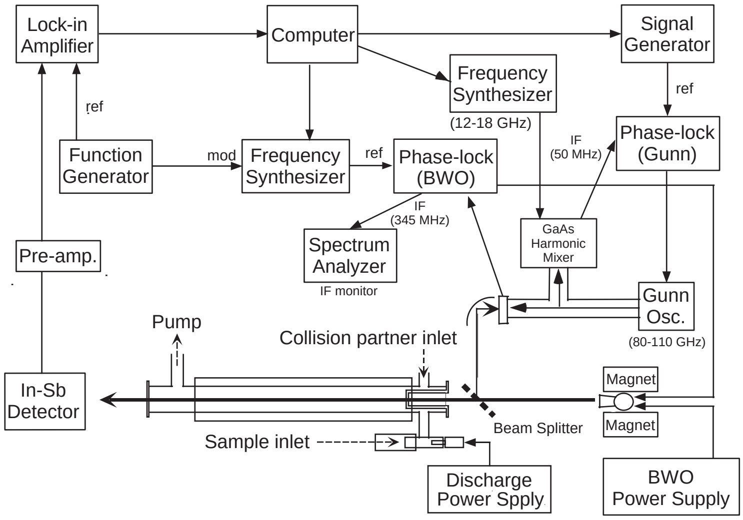

Fig. 1. Block diagram of the Ibaraki submillimeter-wave spectrometer.

dependence of the pressure broadening coefficients is measured while regulating the cell temperature with the low temperature bath circulator. Both ends of the cell are exposed to room temperature. As the radical density is highest at the gas inlet-side of the cell, the exposed portions, in particular, the inlet, cause serious difficulties in determination of the temperature dependence. To alleviate this problem, a "recessed" Teflon window was devised as an inlet side window as shown in Fig. 2. By using this recessed window, the submillimeter-wave beam does not pass through the part of the cell exposed to room temperature. Since the radical concentration is negligibly low at the outlet-side of the cell, the outlet window is a conventional flat Teflon plate. The digital temperature sensors are attached at three different places along the cell length, near the inlet, at the middle point, and near the outlet. The temperature difference among these points is less than 2 K; therefore, their average value is adopted as the cell temperature. These temperature sensors are attached on the surface of the copper jacket. The pressure broadening measurements are carried out after waiting long enough for the temperature of the glass surface and the buffer gas to be equalized with the copper jacket. These BrO measurements cover the temperature range from 224 to 293 K.

A schematic drawing of the cell is illustrated in Fig. 2. In order not to disturb discharge conditions, the sample inlet is separated from the buffer gas inlet, located opposite to the sample inlet. This arrangement prevents buffer gas from flowing into the discharge region. The BrO radical was produced from mixed gas of Br_2 (10 mTorr) and O_2 (40 mTorr) in a DC discharge, with typically 5 mA current, in a side-arm attached to the gas inlet. Sample pressure is monitored by two Baratron (MKS) pressure gauges, one at the inlet and the other at the outlet of the cell. At full pumping speed of a mechanical booster and a rotary pump combination, the pressure gradient through the cell is found to be less than 1%. The discharge current and the flow rate of Br_2 and O_2 through the discharge tube are maintained constant, while the flow rate of the buffer gas (either nitrogen or oxygen) is varied. This procedure assured that the discharge conditions are not altered significantly by varying the buffer gas pressure.

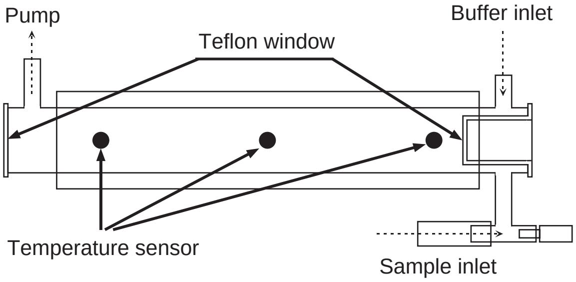

Fig. 2. Schematic diagram of the Ibaraki absorption cell.

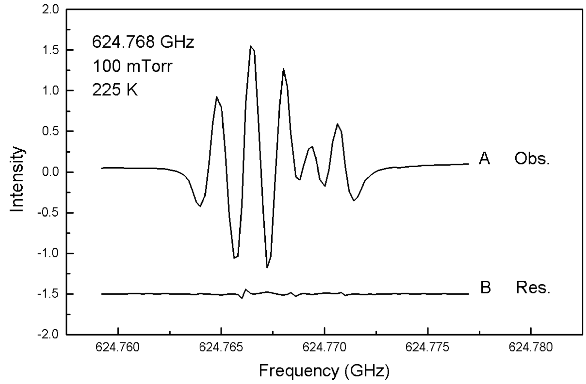

Fig. 3. Ibaraki line profile recorded with 100 mTorr total pressure (Br_2 10 mTorr + O_2 40 mTorr in the discharge region and 50 mTorr of broadening O_2).

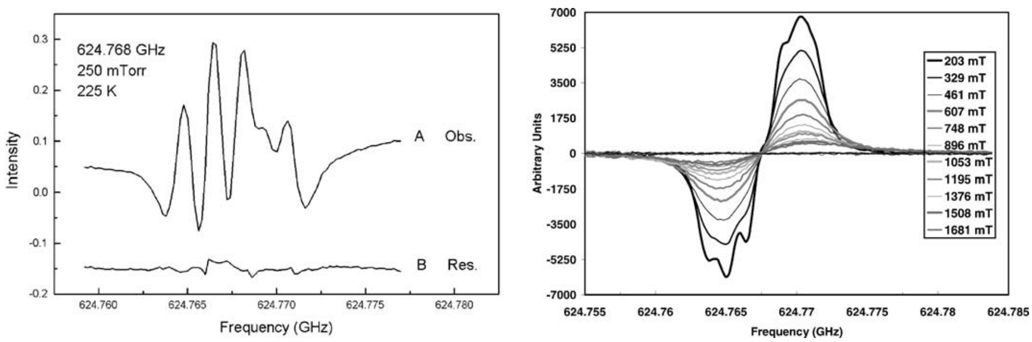

Fig. 4. (Left) Ibaraki line profile recorded with 250 mTorr of O_2 as broadening gas. (Right) JPL room temperature run of BrO in O_2.

Experimental conditions allow measurements with up to 400 mTorr of buffer gas, without disruption of the reaction conditions. At low pressure and low modulation amplitude, the four hyperfine components of $\Delta F = 1$ are resolved, though the Λ-type doubling is barely resolved, even at the lowest pressure used. A typical signal at low pressure is shown in Fig. 3. The signal recorded with Br_2 10 mTorr and O_2 40 mTorr, the lowest pressures used in Ibaraki experiments, was used as a reference signal for the convolution fitting that will be described below in the following section. Fig. 4 (left) shows an example of the signal broadened by adding 200 mTorr of O_2 to the BrO producing DC discharge gas mixture (Br_2 10 mTorr and O_2 40 mTorr), together with the residuals of the fit.

Measurements at JPL are carried out with the submillimeter radiation passed twice through a 1 m length, 7.3 cm diameter, temperature controlled glass cell encapsulated within a glass jacket. The entire experimental design is shown in Fig. 5. A liquid-helium cooled InSb bolometer is used for detection of the first harmonic of the frequency modulated source. The submillimeter radiation at 624 and 650 GHz is produced through successive multiplication of the phase-locked RF source (HP

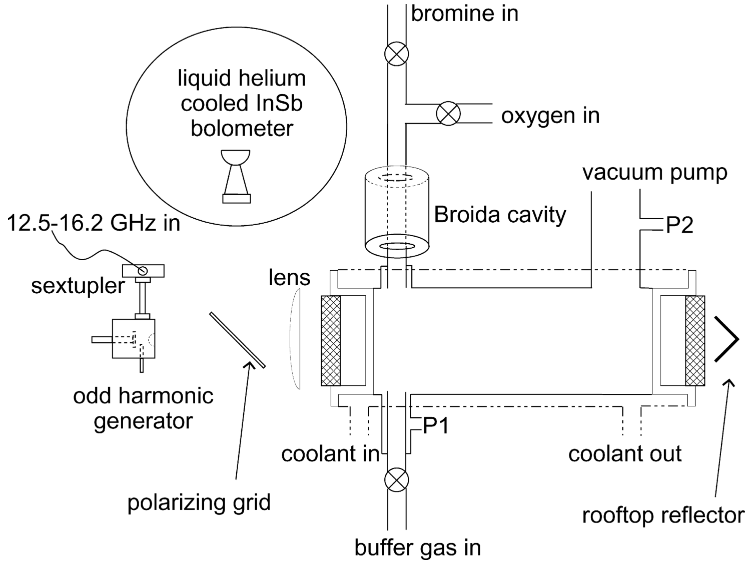

Fig. 5. Experimental setup at JPL for measurement of BrO halfwidths.

8341B). This source is followed by an active sextupler (Millitech) that pumps a JPL-built antiparallel planar Schottky diode multiplier (×7) [8]. The implementation of this multiplier chain (opposed to a phase-locked mm- or sub-mm wave source) provides an easily tunable, stable, synthesized radiation source for performing spectroscopy and halfwidth measurements.

Oxygen and bromine gases are flowed through a microwave discharge cavity located on a quartz side-arm into the free-space spectrometer cell. Best radical production is achieved by combination of the O_2 and Br_2 prior to the discharge at partial pressures of ca. 80 and 10 mTorr, respectively. Similar signal strength could be obtained by combination of the Br_2 after an O_2 discharge. However, this signal was more difficult to stabilize while switching one of the reactants on or off. Using the combined discharge condition, a valve that removes the Br_2 from the flow can be effectively used to remove radicals from the submillimeter beam, and thus allowing background measurement for baseline subtraction without switching the discharge on/off. At the extreme low temperatures condensed Br_2 and bromine oxides often caused residual spectral signatures even with the Br_2 source removed. An elevated level of buffer gas (> 2 Torr) is used to obtain the background scan under these conditions. The buffer gas is flowed into the cell from a port opposite to the discharge.

The spectrometer cell is temperature controlled by flowing liquid nitrogen cooled methanol through a sleeve surrounding the cell. The gases flowing through the cell rapidly thermally equilibrate. Maximum gas flow speeds of ∼24 L/s were found to give more consistent results; no pressure gradient was observed across the flow cell. The temperature is monitored using a pair of 'T'-type thermocouples, one imbedded in the coolant sleeve and the other resting in an ice bath. The coolant temperature can be regulated to within 2 degrees of the desired temperature down to 190 K; however, the BrO condenses on cell walls below 230 K, drastically reducing the available signal for measurement at the extreme temperatures. The lowest temperature pressure broadening measurements at JPL were at 210 K. The teflon windows are inset inside the cooling jacket to minimize thermal gradients in the cell; secondary windows were used to keep atmospheric moisture from condensing on the cold teflon surface. The total pressure is monitored with a calibrated capacitance manometer for accurate determination of the pressures. The pressure gauges showed deviations of less than 1% from actual pressure in a comparison to a standard gauge.

3. Results and analysis

The line profiles are analyzed using a convolution method proposed by Pickett [4]. This method is particularly useful for complicated line profiles such as BrO that have hyperfine and Λ-type splittings. The overlapped hyperfine patterns make absolute fitting of the line profiles difficult. In the convolution method, a lower pressure spectrum is employed as a reference spectrum. The higher pressure spectrum is fitted to a convoluted line profile of the reference signal profile and the additional Lorentzian line profile. Therefore this method assumes that any other contributions to the broadening such as the Doppler broadening and the modulation broadening are constant while changing the buffer gas pressure.

The line profile, $F(i)$, can be described by

$$F(i) = A\sum_{k=1}^{N} R(k)\,\frac{\Delta v^2}{\Delta v^2 + [(i-k)f + s]^2} + a_0 + a_{1i} + a_{2i}^2 + a_{3i}^3 + a_{4i}^4, \quad i = 1, 2, \ldots, n, \tag{1}$$

where $R(k)$ is the line profile of the reference signal, A the amplitude of the signal, Δv the line width(HWHM), f the frequency step size of the scan, s is the pressure shift and N is the number of points in each scan. The polynomial in terms of i in the equation can be used to correct for baseline distortion. The three Lorentzian parameters, Δv, A, and s, are determined from the least-squares analysis along with any baseline corrections. The pressure broadening coefficients and the pressure shifts of the line centers were assumed to be equal for all the hyperfine components of each transition.

In Fig. 6 data from Ibaraki University depicts the Lorentzian halfwidths plotted against pressure at 225 K. Each data point is entered by taking average of 10–70 measurements. The error bars displayed indicate 3σ uncertainty limits. The pressure broadening coefficients were determined by fitting these data to a linear function. In this figure, the halfwidth and the pressure are referred to the reference spectrum.

Measurements made at JPL included scans with no absorber present. Instead of fitting a polynomial for the baseline, the background scans were averaged (before and after) and subtracted from the scan with absorber present. Fig. 4 (right) includes the residuals from fits of the 329–1681 mTorr test spectra with the 203 mTorr spectrum as a reference. Generally, there are no systematic deviations in the residuals of the fitted test spectra. Not shown in Fig. 4 are the residuals of convolution fits with the higher pressure scans as reference spectra. Typically all available data points in a given run were used in determination of a broadening coefficient. Therefore N scans produce $N(N-1)$ (differential halfwidth vs. differential pressure) data points. The slope of this data set gives a single broadening parameter for the temperature of the run. Signal strength depends critically on both temperature and pressure, therefore determining the dynamic range of available linewidth measurements. For each run, broadening gas pressure was increased until $S/N < 20$. Occasionally single scans, usually those with the highest broadening gas pressure and poorest S/N, were removed from the data set. Unreasonable fitting residuals or systematically shifted halfwidths are the general criteria for data removal from the data set.

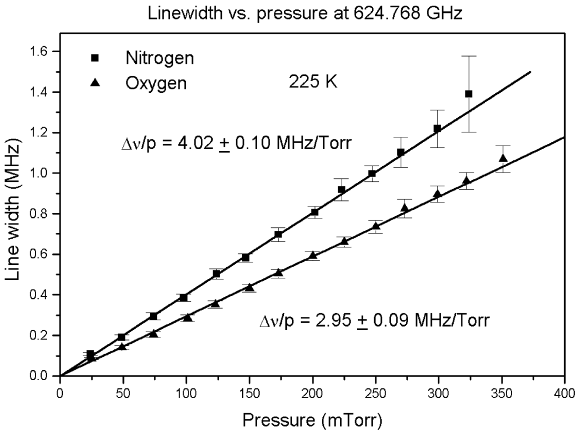

Fig. 6. Pressure induced Lorenztian halfwidths measured at Ibaraki.

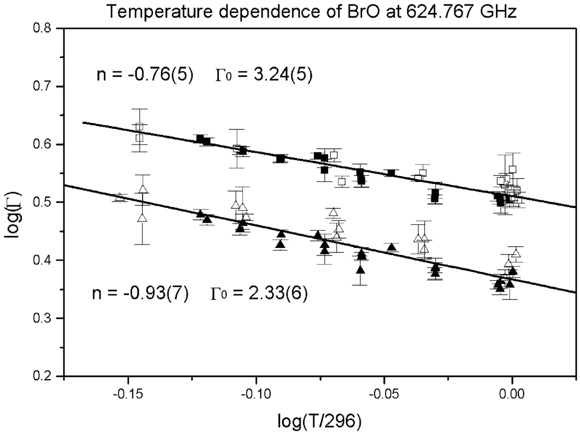

Fig. 7. The temperature dependence of BrO pressure induced halfwidths. Data from JPL (open symbols) and Ibaraki (filled symbols) are depicted. The squares represent N_2 broadening measurements and triangles represent O_2 broadening measurements. The solid lines depict the best fit to the data for each broadening gas.

The fitted parameters represent a difference between the reference and test spectra. A plot of the difference in pressure between the scans vs. the difference in halfwidth determines the broadening coefficient Γ, for the particular temperature of the run (see Fig. 7). No systematic line shifts are determinable from the data sets. Fitted values for the shift parameter fell in a random distribution between ± 100 kHz.

The temperature dependence of pressure broadening parameter is often expressed by

$$\Gamma = \gamma_0 \left(\frac{T}{296} \right)^n, \tag{2}$$

where Γ is pressure broadening coefficient at temperature T, γ_0 the pressure broadening coefficient at 296 K, and n is the temperature exponent. In Fig. 7 the broadening coefficients are plotted against the temperature on a log–log scale. The error bar of each data point represents 3σ. The inverse of each uncertainty for each point was used to weight the data for determination of the final parameters. Best fit lines are drawn for each data set and for the combined data. The precision of the data is 2–3% for each broadening coefficient. Table 1 summarizes the pressure broadening coefficients and their temperature dependence exponents.

The pressure broadening coefficient of BrO is thus determined to be 3.24 ± 0.05 MHz/Torr for the 624.77 GHz line broadened by N_2 with a temperature dependence described by the exponent $n = -0.76 \pm 0.05$. When BrO is perturbed by O_2, the coefficient is found to be 2.33 ± 0.06 MHz/Torr with $n = -0.93 \pm 0.07$ for the same transition. The broadening coefficient that is measured with N_2 for the 650.18 GHz line is 3.20 ± 0.07 MHz/Torr, and O_2 broadening were 2.41 ± 0.06 MHz/Torr (296 K) with temperature dependencies of -0.84 ± 0.07 and -0.70 ± 0.07, respectively.

Table 1
Halfwidth parameters of BrO

Line/gas	624.77 GHz		650.17 GHz	
	γ_0 (MHz/Torr)	n	γ_0 (MHz/Torr)	n
N_2	3.24 (5)	−0.76 (5)	3.20 (7)	−0.84 (7)
O_2	2.33 (6)	−0.93 (7)	2.41 (6)	−0.70 (7)

γ_0 is the pressure broadening coefficient at 296 K, and n is the temperature dependence exponent.

4. Discussion

These investigations are a part of the effort to determine the pressure broadening parameters of BrO for the transitions which are planned to be monitored by the SMILES and EOS-MLS missions.

Signal to noise (S/N) determines the dynamic range of all the halfwidth measurements. Due to system performance issues the S/N ratio was better at 624 GHz compared to 650 GHz in both laboratories. The highest foreign gas pressure used at Ibaraki was about 400 mTorr, while the JPL experiments cover higher pressures up to 1.5 Torr. N_2 pressure broadening, the larger effect of the two buffer gases, is also more difficult to measure due to the decrease in dynamic range (in partial pressure) available for equivalent halfwidths. The two laboratories approached the S/N limitations with different methods. At JPL improved S/N was achieved through the background subtraction technique. At Ibaraki, statistical averaging of multiple measurements was used to improve the quality of the data set. The broadening coefficients obtained by both groups are in reasonable agreement, with some divergence of halfwidth parameters at the lowest temperatures, demonstrating that the data are not seriously biased by systematic errors.

Two other BrO pressure broadening measurements have recently been reported [5,6]. Bauer et al. reported on the $J = 18.5 \leftarrow 17.5$ ^{79}BrO transition at 499.6 GHz. This work reports the air-broadened halfwidth to be 3.54 ± 0.28 MHz/Torr at 296 K with a temperature dependence of -0.45 ± 0.18. The broadening parameters for a higher J transition, $J = 27.5 \leftarrow 26.5$ of ^{81}BrO at 700.97 GHz, were obtained by Fraser [5]. The O_2 pressure broadening coefficient determined in this work is 2.89 ± 0.14 MHz/Torr. The current study reports more precise parameters for intermediate J transitions which are entirely consistent with the literature data and support the generally accepted trend of slowly decreasing halfwidth parameters at elevated J levels in diatomic species.

The dominant interaction which causes the line broadening is the electric quadrupole–electric dipole interaction. The broadening by N_2 is larger than that by O_2. This tendency is similar to that observed for many other molecules. The ratio of the width by N_2 and by O_2 is 1.39 and 1.36 for the 624.77 and 650.17 GHz lines, respectively, while the ratio of the electric quadrupole moments of N_2 and O_2 is about 3.5 [9] (see also references cited therein). The r-dependence of the electric quadrupole–electric dipole interaction is r^{-4}, and the temperature dependence of the pressure broadening in this case is given by [10]

$$\Delta v \propto T^{-5/6} = T^{-0.83} \tag{3}$$

which is in reasonable agreement with our experimental values.

Acknowledgements

The work carried out at Ibaraki University was supported in part by the JEM/SMILES Mission program, Japan Space Forum (The Ground-based Research for Space Utilization Program) and the grants from the Ministry of Education, Science, and Culture(#11694055, #1344017). TA thanks Drs. H. Masuko and Y. Kasai for their constant encouragements. Portions of this paper present research carried out at the Jet Propulsion Laboratory, California Institute of Technology, under contract with the National Aeronautics and Space Administration.

References

[1] Lary DJ. J Geophys Res 1996;101(D1):1505–16.
[2] JEM/SMILES mission plan. Version 2.1, November 15, 2002.
[3] Waters JW, Read WG, Froidevaux L, Jarnot RF, Cofield RE, Flower DA, Lau GK, Pickett HM, Santee ML, Wu DL, Boyles MA, Burke JR, Lay RR, Loo MS, Livesey NJ, Lungu TA, Manney GL, Nakamura LL, Perun VS, Ridenoure BP, Shippony Z, Siegel PH, Thurstans RP, Harwood RS, Pumphrey HC, Filipiak MJ. The UARS and EOS microwave limb sounder (MLS) experiments. J Atmos Sci 1999;56:194.
[4] Pickett HM. Determination of collisional linewidths and shifts by a convolution method. Appl Opt 1980;19:2745.
[5] Fraser HJ. PhD thesis, University of Cambridge, 1998.
[6] Bauer A, Birk M, Wagner G, Colmont JM, Priem D, Wlodarczak G, Buhler S, von Engeln A, Kunzi K, Perrin A. Study on a spectroscopic database for millimeter and submillimeter wavelengths. ESA/ESTEC Contract No. 11581/95/NL/CN final report, 1995.
[7] Amano T, Akao K, Oka H, Unno O. Pressure broadening of O_2 in the $a^1\Delta_g$ state. Chem Phys Lett 1999;311:433–8.
[8] Oswald JE, Koch T, Mehdi I, Pease A, Dengler RJ, Lee TH, Humphrey DA, Kim M, Siegel PH, Frerking MA, Erickson NR. Planar diode solid-state receiver for 557 GHz with state-of-the-art performance. IEEE Microwave and Guided Wave Lett 1998;8:232.
[9] Lawson DB, Harrison JF. Distance dependence and spatial distribution of the molecular quadrupole moments of H_2, N_2, O_2, and F_2. J Phys Chem A 1997;101:4781–92.
[10] Townes CH, Schawlow AL. Microwave spectroscopy. New York: McGraw-Hill, 1955.